

1 Identification and Characterization of Equine Blood Plasmacytoid

2 Dendritic Cells

3

4 Ziegler Anja^a, Marti Eliane^{a*}, Summerfield Artur^{b, c}, Baumann Arnaud^c

5

6 ^a Department of Clinical Research and Veterinary Public Health, Vetsuisse Faculty,

7 University of Bern, Länggassstrasse 124, Bern, Switzerland.

8 ^b Institute of Virology and Immunology, Sensemattstrasse 293, Mittelhäusern, Switzerland.

9 ^c Department of Infectious Diseases and Pathobiology (DIP), Vetsuisse Faculty, University of

10 Bern, Länggassstrasse 122, Bern, Switzerland.

11

12

13 ***Correspondence:** Eliane Marti, Division of Clinical Research, Department of Clinical

14 Research-VPH, Vetsuisse Faculty, University of Bern. Länggassstrasse 124, PO Box 3001

15 Bern, Switzerland.

16 Email: eliane.marti@vetsuisse.unibe.ch

17

18 **Abstract**

19 Dendritic cells (DC) are antigen-presenting cells that can be classified into three major cell
20 subsets: conventional DC1 (cDC1), cDC2 and plasmacytoid DCs (pDC), none of which have
21 been identified in horses. Therefore, the objective of this study was to identify and
22 characterize DC subsets in equine peripheral blood, emphasizing on pDC. Surface marker
23 analysis allowed distinction of putative DC subsets, according to their differential expression
24 of CADM-1 and MHC class II. Equine pDC were found to be Flt3⁺ CD4^{low} CD13⁻ CD14⁻
25 CD172a⁻ CADM-1⁻ MHCII^{low}. The weak expression of CD4 on equine pDC contrasts with
26 findings in several other mammals. Furthermore, pDC purified by fluorescence-activated cell
27 sorting were found to be the only cell subset able to produce large amounts of IFN- α upon
28 TLR9-agonist stimulation. The pDC identity was confirmed by demonstrating high-levels of
29 *PLAC8*, *RUNX2* and *TCF4* expression, showing pDC-restricted expression in other mammals.

30

31 **Keywords:** horse, dendritic cell subset, plasmacytoid dendritic cell.

32

33 **Abbreviations:** ODN, oligodeoxynucleotides; DC, dendritic cells; cDC, conventional DC;
34 FMO, fluorescence minus one; Flt3, fms-like tyrosine kinase 3; Flt3L, Flt3 ligand; IFN,
35 interferon; MoDC, monocyte-derived DC; pDC, plasmacytoid DC; PBMC, peripheral blood
36 mononuclear cells.

37 **1. Introduction**

38 Dendritic cells (DC) represent the professional antigen-presenting cells of the immune system
39 and are essential regulators of immunity and tolerance (Banchereau and Steinman, 1998).
40 They can be further categorized into conventional DC (cDC), which are responsible for
41 antigen presentation and induction of T-cell responses, and plasmacytoid DC (pDC)
42 representing the most potent type I interferon (IFN) producing cell, able to efficiently sense
43 microbial nucleic acid (Liu, 2005). Conventional DC consist of at least two phenotypically
44 distinct subsets stimulating particular T-cell responses (Schlitzer and Ginhoux, 2014). The
45 murine CD8 α ⁺/ human CD141⁺ cells comprise the cDC1 subset, specialized in cross-
46 presentation of antigens to CD8⁺ T-cells and stimulating Th1 immunity (Bachem et al., 2010;
47 Jongbloed et al., 2010). The cDC2 subset was identified as murine CD11b⁺/ human CD1c⁺
48 cells (Haniffa et al., 2013), and is particularly capable to stimulate Th2 and Th17 immunity
49 (Dutertre et al., 2014; Tussiwand and Gautier, 2015). Both pDC and cDC arise from a
50 common DC progenitor in the bone marrow (Liu and Nussenzweig, 2010; Onai et al., 2007)
51 and are dependent on the growth factor fms-like tyrosine kinase 3 ligand (Flt3L) for their
52 development and differentiation (Karsunky et al., 2003; Schmid et al., 2010). Accordingly, all
53 DC subsets express Flt3 receptor (CD135).

54 A number of reports described the presence of distinct cDC subpopulations in veterinary
55 species, including pigs (Guzylack-Piriou et al., 2010; Maisonnasse et al., 2015; Summerfield
56 et al., 2015; Auray et al., 2016, submitted), cattle (Howard et al., 1999; Renjifo et al., 1997)
57 and sheep (Contreras et al., 2010; Pascale et al., 2008). Additionally, pDC have been
58 identified in pig (Summerfield et al., 2003), in cattle (Reid et al., 2011) and in sheep (Pascale
59 et al., 2008).

60 However, neither cDC nor pDC have been described in horses. Studies that have been
61 performed to date, resorted to the use of monocyte-derived dendritic cells (MoDC) (Cavatorta
62 et al., 2009; Mauel et al., 2006; Moyo et al. 2013). Although MoDC possess many functional

63 attributes consistent with DC (Sallusto and Lanzavecchia, 1994), they do not represent *bona*
64 *fide* DC based on their ontogeny. Nevertheless, many *in vivo* studies report MoDC as a
65 distinct subtype of inflammatory monocytic cell, sharing some features with cDC in terms of
66 antigen presentation (Guilliams et al., 2014; Schlitzer et al., 2015). Consequently, for
67 advances in immunological research in horses, it is essential to gain more information on
68 equine *bona fide* DC.

69 The aim of the present study was to phenotypically characterize equine blood DC and
70 functionally identify pDC in healthy horses. As a first step, appropriate cell surface markers
71 which were either equine-specific or shown to cross-react with the equine system were used
72 to identify distinct cell subsets in equine peripheral blood mononuclear cells (PBMC) by flow
73 cytometry. Based on the comparative approach used by Summerfield et al. (2015), a first
74 classification of equine DC subsets is proposed. The identity of purified pDC was further
75 confirmed by a robust IFN- α production upon TLR9-stimulation as well as by a high
76 expression of pDC-specific transcripts.

77

78 **2. Methods**

79 **2.1. Isolation of peripheral blood mononuclear cells from healthy horses**

80 Blood samples were collected from the jugular vein of eleven healthy horses (age = 4 – 21
81 years) using sterile glass bottles supplemented with 5000 I.U./ml heparin (Liquemin[®],
82 Drossapharm AG, Basel, Switzerland) or Sodium-Heparin containing vacutainers (Vacuette[®];
83 Greiner, St.Gallen, Switzerland). The study was approved by the Animal Experimental
84 Committee of the Canton of Berne and Vaud, Switzerland (No. BE 51/13).
85 PBMC were isolated by density gradient centrifugation over Biocoll ($\rho=1.077$ g/ml,
86 Biochrom GmbH, Berlin, Germany) as described (Hamza et al., 2007).

87

88 **2.2. Production of recombinant bovine Flt3 Ligand**

89 Bovine instead of equine Flt3L was used because the complete equine Flt3L gene sequence is
90 still unknown. The partial equine Flt3L sequence (Genbank: XP_005596791.1) exhibits 73%
91 amino acid sequence homology to bovine Flt3L. Bovine Flt3L (NCBI NM_181030.2) was
92 produced as previously described (Guzylack-Piriou et al., 2010) and was originally employed
93 for another study (Baumann et al., unpublished data). Briefly, after deletion of the stop codon,
94 the Flt3L sequence was flanked by HindIII and XbaI restriction sites and was chemically
95 synthesized in pUC57 plasmid (GenScript, Piscataway, NJ, USA). After HindIII and XbaI
96 digestion, Flt3L was ligated in the pEAK8-His expression vector. The TOP10 Chemically
97 Competent *E. coli* cells (Invitrogen, USA) were transformed with the plasmid pEAK8-His
98 containing the bovine Flt3L. For final recombinant production of bovine Flt3L, HEK 293
99 cells were transfected with pEAK8-His-Flt3L using X-tremeGENE 9 following the
100 manufacturer's instructions (Roche, Basel, Switzerland). After 5 days, supernatant was
101 collected and expression of recombinant bovine Flt3L was assessed by western blot using an
102 anti-his-HRP antibody (cat. no. 130-092-785, Miltenyi Biotec; Antibody Register:
103 AB_1103231). The reaction was visualized with a WesternBright ECL Western blotting
104 detection kit (Advansta Inc., Menlo Park, CA, USA) and a CCD-LAS3000 camera (Fuji Film)
105 (Fig. S1).

106

107 **2.3. Surface marker analysis by flow cytometry**

108 PBMC from three horses were transferred to 5ml FACS tubes at 3×10^6 cells per tube. First, a
109 blocking step was performed using Chrome Pure whole mouse IgG (Jackson
110 Immunoresearch, West Grove, PA, USA). All incubations were performed for 20 min on ice,
111 followed by washing with PBS and centrifugation at 500 x g for 5 min. Briefly, cells were
112 incubated with recombinant bovine Flt3L, followed by labelling with a PE-conjugated anti-his
113 antibody (clone GG11-8F3.5.1, cat-no 130-092-691; Miltenyi Biotec; Antibody Register:
114 AB_1103227). Anti-human CADM-1 (cat no. CM004-3, MBL International Corporation;

115 Antibody Registry: AB_592783), shown to specifically bind to the CADM-1 molecule in
116 many mammalian species (Contreras et al., 2010; Dutertre et al., 2014), was detected by a
117 secondary goat biotinylated anti-chicken antibody (cat no 103-065-155, Jackson
118 Immunoresearch; Antibody Registry: AB_2337383), followed by labelling using Brilliant
119 Violet (BV)421 conjugated to Streptavidin (BD Biosciences, Franklin Lakes, NJ, USA).
120 Other surface markers were stained using the following antibodies: anti-equine CD4 (clone
121 CVS4; cat no MCA1078, Bio-Rad; Antibody Register AB_321274), anti-equine CD13 (clone
122 CVS19; cat no MCA1084GA, Bio-Rad; Antibody Registry: AB_321308), anti-equine
123 MHCII (clone CVS20; cat no MCA1085, BioRad; Antibody Register AB_321618), anti-
124 equine CD14 (clone 105; <https://courses2.cit.cornell.edu/wagnerlab/research/reagents.htm>;
125 Kabithe et al., 2010)), anti-bovine CD172a (clone HR-DH59B; cat no HR-BOV2049;
126 Monoclonal Antibody center, Washington State University; Pullman WA, USA) showing
127 cross-reactivity with equine cells (Mérant et al., 2009). These monoclonal antibodies were
128 labelled with mouse IgG1 Alexa Fluor 488, 647 or 700 Zenon labelling kits (Thermo
129 Scientific, Waltham MA, USA). Appropriate isotype and fluorescence-minus-one (FMO)
130 controls were used. Finally, cells were resuspended in phosphate buffered saline (PBS) and
131 analysed on a LSRII flow cytometer (BD Biosciences). Automated compensation for spectral
132 overlap of fluorochromes was calculated by the BD FACSDIVA acquisition software (BD
133 Biosciences) based on single-stained PBMC. Data were analysed using FlowJo software 6
134 (Tree Star Inc. Ashland OR, USA). Gates were set to exclude doublets and lymphocytes
135 based on forward and side scatter characteristics (Fig. 1A). Within this cell population, a
136 further gate was set on Flt3⁺/ CD14^{low} cells, based on isotype and fluorescence minus one
137 (FMO) controls. This gating strategy was used for all flow cytometry experiments.

138

139 **2.4. PBMC stimulation for IFN- α production**

140 PBMC were isolated as described above and suspended in RPMI 1640 medium with HEPES
141 and L-glutamine (Gibco, Life Technologies Ltd, Paisley UK) supplemented with 1%
142 penicillin and streptomycin (Gibco), 1% MEM vitamins, 1% Na pyruvate, 1% Non-essential
143 amino acids (all Biochrom GmbH) and 10% inactivated horse serum (Ziegler et al. 2016, in
144 revision) at a density of 2×10^5 cells per 200 μ l medium in a 96-well round-bottom cell
145 culture plate (Sarstedt, Nümbrecht, Germany). Cells were cultured for 24h in the presence of
146 5 μ g/ml of the synthetic TLR9 agonist Type C CpG-oligodeoxynucleotides (ODN) D-SL03
147 (InvivoGen, San Diego, CA, USA) or of equine herpesvirus-1 (EHV-1; MOI of 0.04 TCID₅₀/
148 cell, EHV1-V144/64, kindly supplied by Prof. Reto Zanoni from the Institute for Virology
149 and Immunology, Vetsuisse Faculty, University of Berne, Switzerland). Thereafter, cell
150 culture supernatants were collected and stored at -80°C until used.

151

152 **2.5. Enrichment of pDC by depletion of PBMC from CD5⁺ and CD14⁺ cells**

153 PBMC were depleted of CD5⁺ and CD14⁺ cells by magnetic separation (MACS technology,
154 Miltenyi Biotec GmbH) according to standard protocols by the manufacturer, using a
155 monoclonal anti-equine CD5 antibody (clone CVS5; cat no MCA1079GA, Bio-Rad;
156 Antibody Register: AB_321382) and anti-equine CD14 (clone 105, Kabithe et al., 2010).
157 Briefly, PBMC were first incubated with anti-CD5 and anti-CD14 simultaneously and, after a
158 washing step, with secondary goat anti-mouse micro beads. Cells were then separated on a
159 LD column (Miltenyi Biotec GmbH). After washing, the CD5/ CD14-depleted (purity > 75%)
160 and CD5/ CD14-enriched (purity > 95%) fraction were stimulated with CpG-ODN or EHV-1
161 as described above for 24h and supernatants were harvested and stored at -80°C until used.

162

163 **2.6. Sorting experiments**

164 Flt3⁺ cells from three horses were enriched from PBMC by MACS separation as described
165 above, using the recombinant bovine Flt3L bound by an anti-his antibody conjugated to PE

166 and ultra-pure anti-PE microbeads (both Miltenyi Biotec GmbH). The magnetic separation
167 was performed at 4°C. Following Flt3-enrichment, cells were stained for expression of CD14,
168 CADM-1 and MHCII as mentioned above. Using a BD FACSAria sorter, Flt3⁺CD14^{low} cells
169 were gated. MHCII^{low}/CADM-1⁻, MHCII^{high}/CADM-1^{low} and MHCII^{high}/CADM-1⁺
170 subpopulations were identified and sorted. Sorted cells were used for subsequent stimulation
171 with the TLR9 agonist CpG-ODN D-SL03, as described above, using 20'000 cells/ 100 µl
172 medium per well. The remaining cells were resuspended in 1ml Isol-RNA Lysis Reagent (5
173 Prime, Hilden, Germany) and kept at -80°C until used.

174

175 **2.7. Equine IFN-α ELISA**

176 For detection of IFN-α in cell culture supernatants, we used an equine IFN-α ELISA (kindly
177 supplied by Dr. Bettina Wagner, Cornell University, Ithaca NY, USA). The assay was
178 performed as described (Wagner et al., 2008). Briefly, anti-IFN-α (clone 29B;
179 <https://courses2.cit.cornell.edu/wagnerlab/research/reagents.htm>) was used for coating of the
180 plates at a concentration of 5 µg/ml. rIFN-α/IgG4 supernatant (85 ng/ml) was serially diluted
181 two-fold, ranging from 42.5 ng/ml – 0.66 ng/ml, to obtain a standard curve. Cell culture
182 supernatants of stimulated cells were tested in duplicates at a 1:2 dilution. For detection,
183 biotinylated anti-IFN-α (clone 240;
184 <https://courses2.cit.cornell.edu/wagnerlab/research/reagents.htm>) was used. This step was
185 followed by incubation with streptavidin-peroxidase and TMB substrate (Sigma-Aldrich
186 GmbH, Buchs, Switzerland). Optical density was measured at 450 nm on an ELISA Reader
187 (BioTek Instruments Inc., Winooski VT, USA) and IFN-α concentration in the samples was
188 calculated according to the standard curve calculated by the Gen5 software (BioTek
189 Instruments Inc.).

190

191 **2.8. Quantitative Reverse-Transcriptase Polymerase Chain Reaction (qRT-PCR)**

192 For RNA extraction from sorted PBMC fractions, 200 μ l of chloroform:IAA (49:1; Sigma-
193 Aldrich GmbH) were added to 1 ml of Isol-RNA lysate and tubes were vigorously shaken by
194 hand. After 5 min incubation at room temperature, samples were centrifuged at 12,000 x g for
195 15 min. The aqueous upper phase was subsequently transferred to a fresh tube and 500 μ l of
196 100% isopropanol were added. Precipitated RNA was then loaded onto a spin column from
197 RNeasy Mini Kit (Qiagen GmbH, Hilden, Germany) and purification was performed
198 according to manufacturer's instructions. RNA was eluted in 40 μ l of RNase-free H₂O. Each
199 sample was quantified spectrophotometrically (NanoDrop 1000, Thermo Scientific) and
200 stored at -80 °C until used. A total of 9 μ l of RNA was employed to synthesize cDNA using
201 GoScript™ Reverse Transcription system (Promega, Madison WI, USA) following
202 manufacturer's instructions. Expression of *PLAC8*, *RUNX2*, *TCF4* and *BACT* were quantified
203 by qPCR using the GoTaq® qPCR Master Mix (Promega) with the primers listed in the table
204 S1. The reaction was performed in a total volume of 25 μ l in the 7500 real-time PCR system
205 (Applied Biosystems, Foster City, CA, USA) under the following fast-cycle amplification
206 conditions: 2 min at 95°C, followed by 40 cycles of denaturation at 95°C for 3 seconds
207 followed by annealing/ extension at 58°C for 30 seconds. The specificity of each primer pair
208 was confirmed in melting-curve analysis and primer efficiency reached > 90% by using serial
209 cDNA dilution as template. Relative expression was normalized to the housekeeping gene
210 *BACT* expression and Δ Ct was calculated as: $2^{-\text{Ct gene}} / 2^{-\text{Ct housekeeping gene}}$.

211

212 **2.9 Statistical Analysis**

213 Statistical analysis was carried out using the software program NCSS8. As the data were not
214 normally distributed, a non-parametric Wilcoxon (signed rank) test was used to compare
215 levels of secreted IFN- α between stimulation conditions. *P*-values ≤ 0.05 were considered
216 significant.

217

218 **3. Results and Discussion**

219 **3.1. Surface marker expression of equine dendritic cell subsets**

220 Since the Flt3 expression on DC is well conserved in mammals (Karsunky et al., 2003;
221 Schmid et al., 2010; Summerfield et al., 2015), Flt3L constitutes a valuable tool to identify
222 DC in a mixed cell population. Orthologous bovine Flt3L was shown to bind to a small
223 heterogeneous population of equine PBMC (0.42 – 0.85%) which did not express CD14 at all,
224 or at very low levels only (Fig 1B).

225 Within the Flt3⁺/ CD14^{low} gate, three subpopulations (P4, P5 and P6) could be further
226 identified based on the differential expression of MHCII and CADM-1 (Fig. 1C). P4 was
227 found to express the lowest levels of CD172a, while P5 expressed high levels, comparable to
228 monocytes (Fig. 1D). None of the subsets was found to express high levels of CD4 (Fig. 1D).
229 Interestingly, CD13 was co-expressed with CADM-1 on a population within Flt3⁺CD14^{low}
230 cells (Fig. 1D). In alignment with other species and considering that CADM-1, CD13, Flt3
231 and CD172a represent cell surface receptors with a species-conserved expression
232 (Summerfield et al., 2015), we propose that equine cDC1 can be identified as Flt3⁺CD4⁻
233 CD13⁺CD14^{low}CD172a⁻CADM-1⁺MHCII^{high} cells, while equine cDC2 would be Flt3⁺CD4⁻
234 CD13⁻CD14^{low}CD172a⁺CADM-1^{low}MHCII^{high}. This will require future confirmation for
235 example by employing transcriptional profiling of the sorted populations. As the present study
236 was focusing on pDC we continued our experimentation focusing on the Flt3⁺CD4⁻ CD13⁻
237 CD14⁻CD172a⁻CADM-1⁻MHCII^{low} subset as a possible candidate for pDC.

238

239 **3.2. Functional identification of equine pDC**

240 As a first experiment, PBMC from eleven healthy horses were stimulated with the synthetic
241 TLR9 agonist type C CpG-ODN or with EHV-1 and the amount of IFN- α in the supernatants
242 was quantified by ELISA. A significant IFN- α induction could be observed in cells stimulated
243 with both EHV-1 and CpG-ODN compared to unstimulated cells (Fig.2A). Intriguingly, while

244 an induction of IFN- α by EHV-1 was shown in PBMC from all horses, five out of the eleven
245 tested horses were non-responsive to stimulation by CpG-ODN (Fig. 2A). The strongest
246 induction of IFN- α in response to CpG-ODN was detectable with PBMC of horses, which
247 also released the highest quantities of IFN- α in response to EHV-1. We speculate that there
248 was a higher number of pDC present in the PBMC of these horses. On the other hand, EHV-1
249 contains a number of pathogen-associated molecular patterns. It may have been able to induce
250 IFN- α production through a broader stimulation of various pathways, possibly also in other
251 cells than pDC, thus inducing IFN- α secretion also in PBMC of horses which were
252 unresponsive to CpG-ODN stimulation. In order to enrich the pDC population, PBMC were
253 depleted of CD5⁺ T-cells and CD14⁺ monocytes. Whereas CD5⁻/CD14⁻depleted PBMC
254 released high levels of IFN- α , no response was observed in CD5⁻/CD14⁻enriched fractions
255 after CpG or virus stimulation (Fig. S2). These data indicate that the pDC do not express CD5
256 and CD14.

257 To further confirm pDC identity and to obtain sufficient cell numbers for FACS sorting, Flt3⁺
258 cells were enriched by MACS sorting, resulting in 7% Flt3⁺ cells (range 3 – 10.1%), which
259 represented an 11-fold enrichment (data not shown). Similar to what we observed with
260 PBMC, three cell subsets could be clearly distinguished in the CD14^{low}/ Flt3⁺ fraction with
261 regard to MHCII and CADM-1 expression (Fig. 2B). They were subsequently sorted by
262 FACS. Stimulation of PBMC, Flt3 MACS-enriched and Flt3 MACS-depleted fractions with
263 CpG-ODN revealed distinct differences in IFN- α induction, confirming the presence of pDC
264 in the Flt3⁺ cells (Fig. 2C). Slight increase in IFN- α secretion was observed in the Flt3
265 MACS-enriched compared to PBMC (median; range = 14.1; 9.1 – 22.2 ng/ml and 9.7; 0.23 –
266 11.9 ng/ml, respectively), whereas no IFN- α production could be detected in the Flt3-depleted
267 fraction. As hypothesized, IFN- α was solely produced by the P4 fraction of putative pDC
268 (median 20.2; range 15.9 – 50.3 ng/ml), with no IFN- α production detected in the other two
269 subsets, indicating that the P4 subset would represent pDC.

270 Recent breakthroughs in transcriptomic profiling of DC subsets have revealed cell-type
271 specific transcripts some of which were conserved between species (Miller et al., 2012; Shay
272 et al. 2013). Thus, new possibilities have opened up for characterization of DC subsets in
273 veterinary species (Summerfield et al., 2015; Vu Manh et al., 2015). Moreover, expression
274 analysis of genes known to be specifically expressed in pDCs in other species including
275 *PLAC8* (=C-15) (Rissoan et al., 2002), *RUNX2* (Sawai et al., 2013) and *TCF4* (= E2-2) (Cisse
276 et al., 2008) revealed a high expression in the putative equine pDC fraction (Fig. 2D). While
277 *RUNX2* levels were found to be low in the P5 cell fraction, no expression of the other
278 transcripts was detected, indicating that *PLAC8* and *TCF4* represent pDC-specific transcripts
279 also in horses. We found a similar restricted expression of these genes in porcine pDC (Auray
280 and Summerfield, unpublished results). While the function of *PLAC8* on pDC is unknown,
281 *RUNX2* and in particular *TCF4* represent essential transcription factors for their development
282 (Sawai et al., 2013; Cisse et al., 2008). Considering the transcriptions factors controlling
283 immune cell development are well conserved, this data confirms that the Flt3⁺CD4⁻ CD13⁻
284 CD14⁻CD172a⁻CADM-1⁻MHCII^{low} P4 subset represents or contains equine pDC.

285 In summary, we have identified equine pDC and propose a basis for further characterization
286 of equine blood cDC. Alignment of the phenotype of equine pDC with other species
287 highlighted some intriguing differences, such as a very low or lacking expression of CD4,
288 contrasting with several other mammals (Summerfield et al., 2015). Considering the
289 importance of DC in many immunological processes, future work should follow to identify
290 DC-subset specific transcripts, which will be the basis to establish reagents for equine DC
291 characterization.

292

293 **4. Conflicts of interest**

294 The authors declare no conflicts of interest

295

296 **5. Acknowledgements**

297 We are grateful to Dr. Andreas Zurbriggen, Department of Clinical Research and Veterinary
298 Public Health, Vetsuisse Faculty, University of Bern for his continuous support. We would
299 like to thank Dr. Bettina Wagner at the Department of Population Medicine and Diagnostic
300 Sciences, College of Veterinary Medicine, Cornell University, Ithaca, NY 14853, USA for
301 providing the anti-equine CD14 antibody and the equine IFN- α ELISA, as well as Prof. Reto
302 Zanoni at the Institute for Virology and Immunology, Vetsuisse Faculty, University of Berne,
303 Switzerland for supplying the EHV-1.

304

305 **6. Funding**

306 This work was supported by a grant of the Department of Clinical Research VPH, Vetsuisse
307 Faculty, University of Bern and by the Swiss National Science Foundation grant no. 310030-
308 160196/1. The support was purely financial, the funding sources were not involved in the
309 collection or analysis of data, in the writing of the manuscript, nor in the decision to submit
310 the article for publication.

311 **7. References**

- 312 Bachem, A., Güttler, S., Hartung, E., Ebstein, F., Schaefer, M., Tannert, A., Salama, A.,
313 Movassaghi, K., Opitz, C., Mages, H.W., Henn, V., Kloetzel, P.M., Gurka, S., Kroczeck,
314 R.A., 2010. Superior antigen cross-presentation and XCR1 expression define human
315 CD11c+ CD141+ cells as homologues of mouse CD8+ dendritic cells. *J. Exp. Med.* 207(6),
316 1273-81.
- 317 Banchereau, J., Steinman, R.M., 1998. Dendritic cells and the control of immunity. *Nature.*
318 392(6673), 245-52.
- 319 Cavatorta, D.J., Erb, H.N., Flaminio, M.J., 2009. Ex vivo generation of mature
320 equinemonocyte-derived dendritic cells. *Vet. Immunol. Immunopathol.* 131(3-4), 259-67.
- 321 Cisse, B., Caton, M.L., Lehner, M., Maeda, T., Scheu, S., Locksley, R., Holmberg, D.,
322 Zweier, C., den Hollander, N.S., Kant, S.G., Holter, W., Rauch, A., Zhuang, Y., Reizis, B.
323 2008. Transcription factor E2-2 is an essential and specific regulator of plasmacytoid
324 dendritic cell development. *Cell.* 135(1), 37-48.
- 325 Contreras, V., Urien, C., Guiton, R., Alexandre, Y., Vu Manh, T.P., Andrieu, T., Crozat, K.,
326 Jouneau, L., Bertho, N., Epardaud, M., Hope, J., Savina, A., Amigorena, S., Bonneau, M.,
327 Dalod, M., Schwartz-Cornil, I., 2010. Existence of CD8 α -like dendritic cells with a
328 conserved functional specialization and a common molecular signature in distant mammalian
329 species. *J. Immunol.* 185(6), 3313-25.
- 330 Dutertre, C.A., Wang, L.F., Ginhoux, F., 2014. Aligning bona fide dendritic cell populations
331 across species. *Cell. Immunol.* 291(1-2), 3-10.
- 332 Guilliams, M., Ginhoux, F., Jakubzick, C., Naik, S.H., Onai, N., Schraml, B.U., Segura, E.,
333 Tussiwand, R., Yona, S., 2014. Dendritic cells, monocytes and macrophages: a unified
334 nomenclature based on ontogeny. *Nat. Rev. Immunol.* 14(8), 571-8.

335 Guzylack-Piriou, L., Alves, M.P., McCullough, K.C., Summerfield, A., 2010. Porcine Flt3
336 ligand and its receptor: generation of dendritic cells and identification of a new marker for
337 porcine dendritic cells. *Dev. Comp. Immunol.* 34(4), 455-64.

338 Hamza, E., Doherr, M.G., Bertoni, G., Jungi, T.W., Marti, E., 2007. Modulation of allergy
339 incidence in icelandic horses is associated with a change in IL-4-producing T cells. *Int. Arch.*
340 *Allergy. Immunol.* 144(4), 325-37.

341 Haniffa M, Collin M, Ginhoux F. Ontogeny and functional specialization of dendritic cells in
342 human and mouse. *Adv. Immunol.* 2013; 120:1-49. Review.

343 Howard, C.J., Brooke, G.P., Werling, D., Sopp, P., Hope, J.C., Parsons, K.R., Collins, R.A.,
344 1999. Dendritic cells in cattle: phenotype and function. *Vet. Immunol. Immunopathol.* 72(1-
345 2), 119-24.

346 Jongbloed, S.L., Kassianos, A.J., McDonald, K.J., Clark, G.J., Ju, X., Angel, C.E., Chen, C.J.,
347 Dunbar, P.R., Wadley, R.B., Jeet, V., Vulink, A.J., Hart, D.N., Radford, K.J., 2010. Human
348 CD141+ (BDCA-3)+ dendritic cells (DCs) represent a unique myeloid DC subset that cross-
349 presents necrotic cell antigens. *J. Exp. Med.* 207(6), 1247-60.

350 Kabithe, E., Hillegas, J., Stokol, T., Moore, J., Wagner, B., 2010. Monoclonal antibodies to
351 equine CD14. *Vet. Immunol. Immunopathol.* 138(1-2), 149-53

352 Karsunky, H., Merad, M., Cozzio, A., Weissman, I.L., Manz, M.G., 2003. Flt3 ligand
353 regulates dendritic cell development from Flt3+ lymphoid and myeloid-committed
354 progenitors to Flt3+ dendritic cells in vivo. *J. Exp. Med.* 198(2), 305-13.

355 Liu, Y.J., 2005. IPC: professional type 1 interferon-producing cells and plasmacytoid
356 dendritic cell precursors. *Annu. Rev. Immunol.* 23, 275-306.

357 Liu, K., Nussenzweig, M.C., 2010. Origin and development of dendritic cells. *Immunol. Rev.*
358 234(1), 45-54.

359 Maisonnasse, P., Bouguyon, E., Piton, G., Ezquerro, A., Urien, C., Deloizy, C., Bourge, M.,
360 Leplat, J.J., Simon, G., Chevalier, C., Vincent-Naulleau, S., Crisci, E., Montoya, M.,
361 Schwartz-Cornil, I., Bertho, N., 2015. The respiratory DC/macrophage network at steady-
362 state and upon influenza infection in the swine biomedical model. *Mucosal Immunol.* Epub
363 ahead of print.

364 Mael, S., Steinbach, F., Ludwig, H., 2006. Monocyte-derived dendritic cells from horses
365 differ from dendritic cells of humans and mice. *Immunology.* 117(4), 463-73.

366 Mérant, C., Breathnach, C.C., Kohler, K., Rashid, C., Van Meter, P., Horohov, D.W., 2009.
367 Young foal and adult horse monocyte-derived dendritic cells differ by their degree of
368 phenotypic maturity. *Vet. Immunol. Immunopathol.* 131(1-2), 1-8.

369 Miller, J.C., Brown, B.D., Shay, T., Gautier, E.L., Jojic, V., Cohain, A., Pandey, G., Leboeuf,
370 M., Elpek, K.G., Helft, J., Hashimoto, D., Chow, A., Price, J., Greter, M., Bogunovic, M.,
371 Bellemare-Pelletier, A., Frenette, P.S., Randolph, G.J., Turley, S.J., Merad, M., 2012.
372 Immunological Genome Consortium. Deciphering the transcriptional network of the
373 dendritic cell lineage. *Nat. Immunol.* 13(9), 888-99.

374 Moyo, N.A., Marchi, E., Steinbach, F., 2013. Differentiation and activation of equine
375 monocyte-derived dendritic cells are not correlated with CD206 or CD83 expression.
376 *Immunology.* 139(4), 472-83.

377 Onai, N., Obata-Onai, A., Schmid, M.A., Ohteki, T., Jarrossay, D., Manz, M.G., 2007.
378 Identification of clonogenic common Flt3⁺M-CSFR⁺ plasmacytoid and conventional
379 dendritic cell progenitors in mouse bone marrow. *Nat. Immunol.* 8(11), 1207-16.

380 Pascale, F., Contreras, V., Bonneau, M., Courbet, A., Chilmonczyk, S., Bevilacqua, C.,
381 Epardaud, M., Niborski, V., Riffault, S., Balazuc, A.M., Foulon, E., Guzylack-Piriou, L.,
382 Riteau, B., Hope, J., Bertho, N., Charley, B., Schwartz-Cornil, I., 2008. Plasmacytoid
383 dendritic cells migrate in afferent skin lymph. *J. Immunol.* 180(9), 5963- 72.

384 Reid, E., Juleff, N., Gubbins, S., Prentice, H., Seago, J., Charleston, B., 2011. Bovine
385 plasmacytoid dendritic cells are the major source of type I interferon in response to foot-
386 and-mouth disease virus in vitro and in vivo. *J. Virol.* 85(9), 4297-308.

387 Renjifo, X., Howard, C., Kerkhofs, P., Denis, M., Urbain, J., Moser, M., Pastoret, P.P., 1997.
388 Purification and characterization of bovine dendritic cells from peripheral blood. *Vet.*
389 *Immunol. Immunopathol.* 60(1-2), 77-88.

390 Rissoan, M.C., Duhon, T., Bridon, J.M., Bendriss-Vermare, N., Péronne, C., de Saint, Vis, B.,
391 Brière, F., Bates, E.E., 2002. Subtractive hybridization reveals the expression of
392 immunoglobulin-like transcript 7, Eph-B1, granzyme B, and 3 novel transcripts in human
393 plasmacytoid dendritic cells. *Blood.* 100(9), 3295-303.

394 Sallusto, F., Lanzavecchia, A., 1994. Efficient presentation of soluble antigen by cultured
395 human dendritic cells is maintained by granulocyte/macrophage colony-stimulating factor
396 plus interleukin 4 and downregulated by tumor necrosis factor alpha. *J. Exp. Med.* 179(4),
397 1109-18.

398 Sawai, C.M., Sisirak, V., Ghosh, H.S., Hou, E.Z., Ceribelli, M., Staudt, L.M., Reizis, B.,
399 2013. Transcription factor Runx2 controls the development and migration of plasmacytoid
400 dendritic cells. *J. Exp. Med.* 210(11), 2151-9.

401 Schlitzer, A., Ginhoux, F., 2014. Organization of the mouse and human DC network. *Curr.*
402 *Opin. Immunol.* 26, 90-9.

403 Schlitzer, A., McGovern, N., Ginhoux, F., 2015. Dendritic cells and monocyte-derived cells:
404 Two complementary and integrated functional systems. *Semin. Cell. Dev. Biol.* 41, 9- 22.

405 Schmid MA, Kingston D, Boddupalli S, Manz MG. Instructive cytokine signals in dendritic
406 cell lineage commitment. *Immunol Rev.* 2010; 234(1):32-44.

407 Shay, T., Jojic, V., Zuk, O., Rothamel, K., Puyraimond-Zemmour, D., Feng, T., Wakamatsu,
408 E., Benoist, C., Koller, D., Regev, A., 2013. ImmGen Consortium. Conservation and
409 divergence in the transcriptional programs of the human and mouse immune systems. *Proc.*
410 *Natl. Acad. Sci. USA.* 110(8), 2946-51.

411 Summerfield, A., Guzylack-Piriou, L., Schaub, A., Carrasco, C.P., Tâche, V., Charley, B.,
412 McCullough, K.C., 2003. Porcine peripheral blood dendritic cells and natural interferon-
413 producing cells. *Immunology.* 110(4), 440-9.

414 Summerfield, A., Auray, G., Ricklin, M., 2015. Comparative dendritic cell biology of
415 veterinary mammals. *Annu. Rev. Anim. Biosci.* 3, 533-57.

416 Tussiwand, R., Gautier, E.L., 2015. Transcriptional Regulation of Mononuclear Phagocyte
417 Development. *Front. Immunol.* 2015. 6, 533.

418 Vu Manh, T.P., Bertho, N., Hosmalin, A., Schwartz-Cornil, I., Dalod, M., 2015. Investigating
419 Evolutionary Conservation of Dendritic Cell Subset Identity and Functions. *Front.*
420 *Immunol.* 6, 260.

421 Wagner, B., Hillegas, J.M., Flaminio, M.J., Watrang, E., 2008. Monoclonal antibodies to
422 equine interferon-alpha (IFN-alpha): new tools to neutralize IFN-activity and to detect
423 secreted IFN-alpha. *Vet. Immunol. Immunopathol.* 125(3-4), 315-25.

424

425

426 **Figure Legends**

427 **Figure 1.**

428 Phenotype of Flt3⁺ cells in equine PBMC. (A) Gating strategy to remove doublets and include
429 FSC^{high}/SSC^{high} large cells. A total number of 250³000 cells were acquired. (B) Within the
430 single, large cell gate, based on the fluorescence minus one (FMO) control, a gate on
431 Flt3⁺CD14⁻ cells was set. (C) Identification of three putative DC subpopulations based on
432 MHCII and CADM-1 expression within Flt3⁺CD14⁻ gated cells. (D) Histograms showing the
433 expression levels of CD172a, CD4 and CD13 in P4 (red; pDC), P5 (blue; cDC2) and P6
434 (orange; cDC1) compared to PBMC (grey). Data are shown for one representative animal out
435 of three.

436

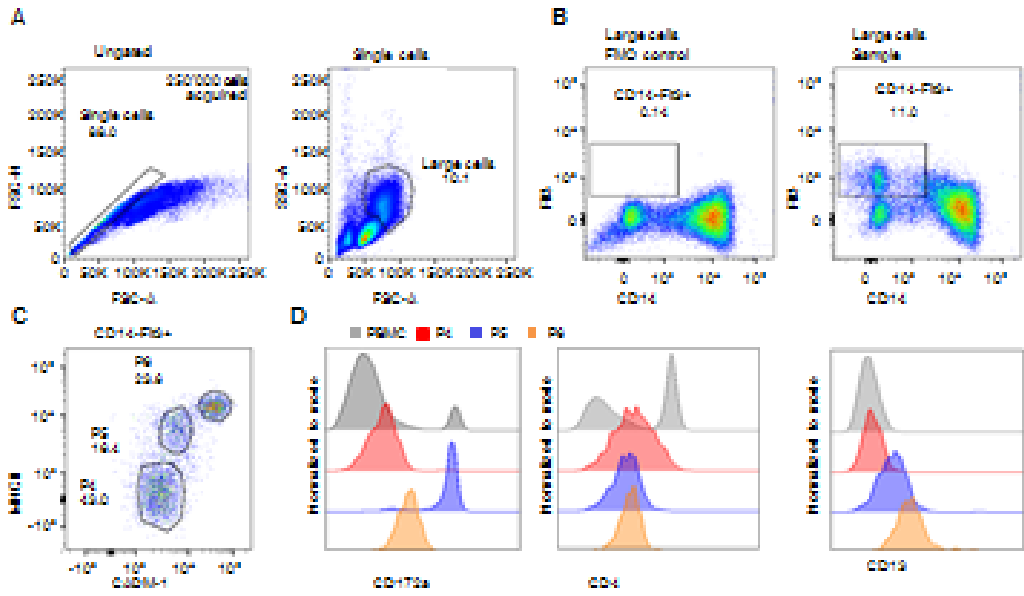
437 **Figure 2.**

438 Characterization of equine pDC. (A) IFN- α secretion by equine PBMC upon stimulation with
439 CpG-ODN (5 μ g/ml) or EHV-1 (MOI of 0.04 TCID₅₀/cell). Samples were tested in duplicates
440 and results are displayed as mean optical density (OD) measured at 450 nm. Each symbol
441 indicates a separate horse with red lines indicating the median. A non-parametric paired
442 sample Wilcoxon signed rank test was performed to compare the stimulation conditions. P-
443 values ≤ 0.05 were considered statistically significant as indicated by asterisks. (B) Gating
444 strategy of putative DC subsets within Flt3-enriched cells which were employed for FACS. A
445 gate was set on the Flt3⁺/CD14^{low} cells. The three distinct cell populations in the CADM-1/
446 MHCII plot were then gated and sorted. (C) IFN- α was detected in cell culture supernatants of
447 PBMC (white background), Flt3-enriched and Flt3-depleted fractions, respectively (light
448 green background) as well as FACS-sorted DC subsets (red background) stimulated with 5
449 μ g/ml CpG-ODN for 24h. Each symbol represents an individual horse with red lines
450 indicating the median. Samples were tested in duplicates and results are displayed as ng/ml.
451 (D) Relative expression of *PLAC8*, *RUNX2* and *TCF4* transcripts in the sorted populations P4,

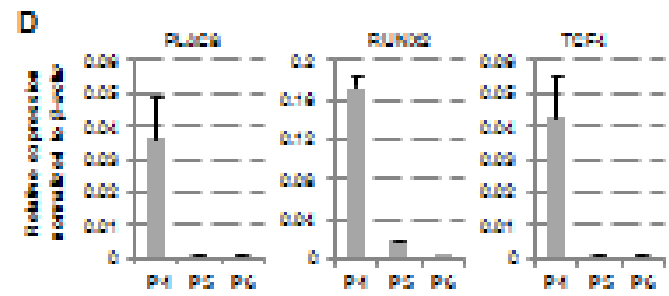
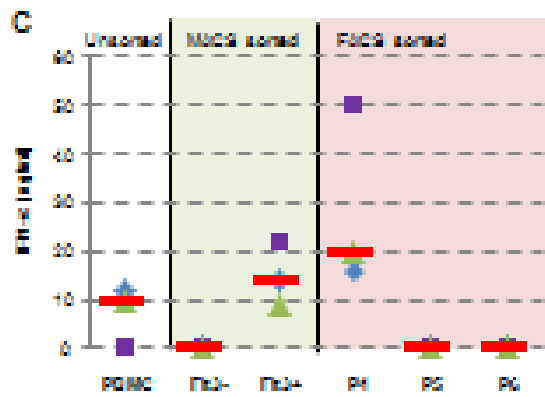
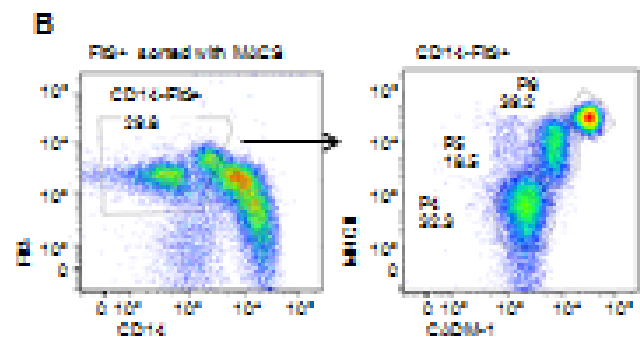
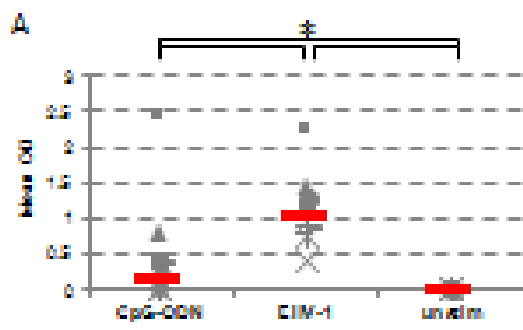
452 P5 and P6. The expression was normalized to the housekeeping gene *BACT*. Bars show the
453 mean \pm SD of an independent experiment performed in duplicate. One representative sorting
454 out of three is shown.

455

456



457
458



459

460

461 **Table S1.** Primers used for qRT-PCR.

Transcription Factor Gene	Primer	Sequence
<i>PLAC8</i>	Forward	5' GCCAGTGGTCATTGTGACTC
	Reverse	5' GATCCAGGGATGCCATATCG
<i>RUNX2</i>	Forward	5' GGCAAGAGTTTCACCTTGAC
	Reverse	5' GAATGCGCCCTAAATCACTG
<i>TCF4</i>	Forward	5' CCACCTCAAGAGTGACAAAC
	Reverse	5' TTTCAGACACGCAGCTTTCG
<i>BACT</i>	Forward	5' CACCACACCTTCTACAAC
	Reverse	5' ATCTGGGTCATCTTCTCG

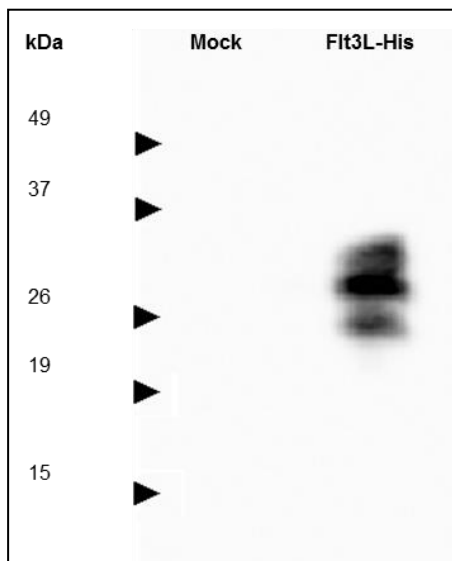
462

463 **Table S2.** Proposed classification of equine dendritic cell subsets in the blood based on
464 surface marker expression.

DC subset	Flt3	CD4	CD14	CD172a	CD13	CADM-1	MHCII
cDC1	+	-	(-)	-	+	+	++
cDC2	+	-	(-)	+	-	-	++
pDC	+	(-)	-	-	-	-	+

465
466
467
468
469

470 **Figure S1.** Recombinant bovine Flt3L expressed in HEK293 cells was visualized by Western
471 blotting. A total of 20 µl of 10-fold diluted supernatant was loaded on the gel. The Flt3L was
472 detected with an mouse anti-His-HRP antibody (Miltenyi Biotec, Antibody Register:
473 Antibody Register: AB_1103231) and visualized with a WesternBright ECL Western blotting
474 detection kit (Advansta Inc., Menlo Park, CA, USA)



475
476